Near-infrared multispectral endoscopic imaging of deep artificial interproximal lesions in extracted teeth

Yaxuan Zhou, a,b Robert C. Lee, Sara Finkleman, Alizera Sadr, Eric J. Seibela,b,c,*

- ^a Univ. of Washington, Human Photonics Lab, Mechanical Engineering, 4000 Mason St, Seattle, USA, 98195
- ^b Univ. of Washington, Dept. of Electrical and Computer Engineering, 185 E Stevens Way NE, Seattle, USA, 98195
- ^c Univ. of Washington, School of Dentistry, 1959 NE Pacific St, Seattle, USA, 98195

Background and Objective: A safer alternative method to radiographic imaging is needed. We present a multispectral near-infrared scanning fiber endoscope (nirSFE) for dental imaging which is designed to be the smallest imaging probe with near-infrared (NIR) imaging (1200-2000nm).

Materials and Methods: The prototype nirSFE is designed for wide-field forward viewing of scanned laser illumination at 1310, 1460, or 1550 nm. Artificial lesions with varying sizes and locations were prepared on proximal surfaces of extracted human teeth to examine capability and limitation of this new dental imaging modality. Nineteen artificial interproximal lesions and several natural occlusal lesions on extracted teeth were imaged with nirSFE, OCT and microCT.

Results: Our nirSFE system has a flexible shaft as well as a probe tip with diameter of 1.6mm and a rigid length of 9mm. The small form factor and multispectral NIR imaging capability enables multiple viewing angles and reliable detection of lesions that can extend into the dentin. Among nineteen artificial interproximal lesions, the nirSFE reflectance imaging operating at 1460-nm and OCT operating at 1310-nm scanned illumination exhibited high sensitivity for interproximal lesions that were closer to occlusal surface. Diagnosis from a non-blinded trained user by looking at real-time occlusal-side nirSFE videos indicate true positive rate of 78.9%. There were no false positives. Conclusions: This study demonstrates that nirSFE may be used for detecting occlusal lesions and interproximal lesions located less than 4 mm under the occlusal surface. Major advantages of this imaging system include multiple viewing angles due to flexibility and small form factor, as well as the ability to capture real-time video. The multispectral nirSFE has the potential to be employed as a low-cost dental camera for detecting dental lesions without exposure to ionizing radiation.

Keywords: dental imaging, near infrared imaging, artificial lesion, optical coherence tomography (OCT), micro computed tomography (μ CT).

*Eric J. Seibel, E-mail: eseibel@uw.edu

1 Introduction

Dental caries can cause pain and can lead to systemic problems, negatively impacting quality of life and resulting in significant economic and social burden on individuals and families¹. Coronal carious lesions are generally formed in a process initiated by loss of minerals due to a shift in the dynamic balance between demineralization and remineralization of enamel. This happens in the acidic environment generated by cariogenic bacteria biofilms metabolizing dietary carbohydrates. The current gold-standard clinical technique for detecting carious lesions is the two-dimensional bitewing x-ray imaging, which is interpreted in combination with visual inspection under adequate

light and magnification. Limitations of the radiographs include image artifacts, lack of quantification and risk for ionizing radiation to patients and clinicians². Interproximal lesions and occlusal lesions are the two most common types of lesions. And they can be difficult to detect using visual, tactile and radiographic examinations. Thus there is a need for a safer alternative method to radiographic imaging for caries detection.

Over the past 40 years, there has been continuous effort on developing new imaging modalities for dental diagnosis³⁻⁶. Among various methods, near-infrared (NIR) optical imaging has great potential. Specifically, in the wavelength range of 1200-1800 nm, NIR light has over 20x lower attenuation coefficient μ_a (e.g. 2-3 cm⁻¹ at 1310 nm) in healthy enamel than visible light (e.g. 60 cm⁻¹ at 632 nm) as well as lower water absorption coefficient than longer wavelength⁷⁻⁹, as shown in Fig. 1. Importantly, μ_a increases with more mineral loss from demineralization due to higher NIR light scattering¹⁰. Thus, carious lesions can appear brighter in NIR reflectance imaging since NIR light is scattered by lesions¹¹⁻¹⁴. Additionally, NIR wavelength is more transparent to stains and non-calcified plaque which can lead to false-positive errors during visual examination and fluorescence-based imaging modalities^{6, 15}. High lesion contrast has been demonstrated in vitro using NIR-sensitive cameras based on InGaAs sensor¹⁶. However, the smallest available NIR MQ022HG-IM-SM5X5-NIR (XIMEA, Münster, Germany) has size camera of 26mm×26mm×31mm. This large form factor is undesirable for patients, especially for pediatric patients.

In this report, we present the first near-infrared scanning fiber endoscope (nirSFE) with advantages of miniature probe size, expected low cost as well as real-time video with good quality. The nirSFE provides a multispectral NIR beam of light that is scanned to form high frame-rate images from a miniature probe with diameter of 1.6mm, which is nearly the diameter of a round toothpick. The

nirSFE fiber-coupled light sources and point detectors are low in cost as they are routinely used in telecommunications, at laser wavelengths of 1.31 to 1.55 μ m. In order to compare to existing and emerging dental imaging systems, artificial interproximal lesions are created on extracted human teeth, and the nirSFE images are analyzed in comparison to the microCT images and the OCT system at the School of Dentistry, University of Washington.

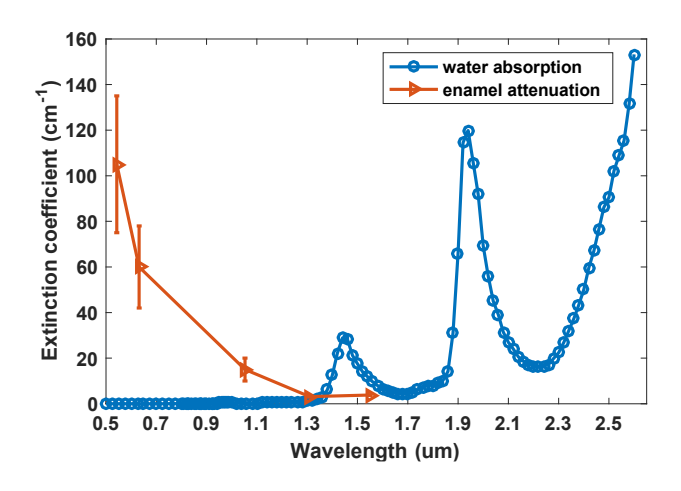


Fig. 1 Attenuation coefficient of light in dental enamel layer and water⁷⁻⁹.

2 Instrumentation

As shown in Fig. 2(a), a cantilevered single-mode optical fiber (SM1250G80, Thorlabs Inc., Newton, NJ) is attached to a quartered piezo tube actuator by epoxy adhesive and then mounted in a collar, which is encapsulated along with the lens assembly inside the scanner housing. Several multi-mode return fibers surround the scanner housing and are protected by an outer sheath. When the four piezo tube electrodes apply sinusoidal signals with phase difference on the actuator, the central illumination fiber is driven to scan in a spiral pattern. As signal amplitude increases, the spiral expands so that the active scanning of the laser beam covers the whole field of view (FOV) whose size is determined by the resonance deflection amplitude of the scanning fiber as well as magnification of the lens assembly fixed in front of the scanning fiber. Meanwhile, the back-

scattered light is collected non-confocally through fibers into a point detector whose output is mapped onto the final image. The SFE scope has diameter of 1.6mm and a rigid length of 9 mm, which is over 800 times smaller in volume than the smallest commercial InGaAs camera.

We are using the standard scanning cantilever with a length of \sim 2.27 mm and primary resonance frequency of \sim 11KHz in nirSFE probe. The maximum deflection amplitude during scanning is $\pm \frac{1}{4}$ mm. The number of scan spirals per frame is typically 250. Electronic system has detection sampling rate of 10 MSps (Mega samples per second) and frame rate of 7Hz which is determined by resonance frequency and number of scan spirals per frame, and can reach 20Hz but is currently limited by the FPGA board (USB-7856R, National Instruments Corp., Austin, TX). Typical working distance from SFE tip to tooth is 20 mm to view an entire tooth surface, and depth of field is even greater since the scanned beam is nearly collimated. We use laser diodes with wavelength 1310 nm (LPSC-1310-FC, Thorlabs Inc., Newton, NJ), 1460 nm (QFBGLD-1460-150, Thorlabs Inc., Newton, NJ) and 1550 nm (FPL1009S, Thorlabs Inc., Newton, NJ) and power of around 50mW in ex-vivo imaging experiments for optimal image quality. The NIR optical detection is achieved by using ten multimode collection fibers (FP200ERT, Thorlabs Inc., Newton, NJ).

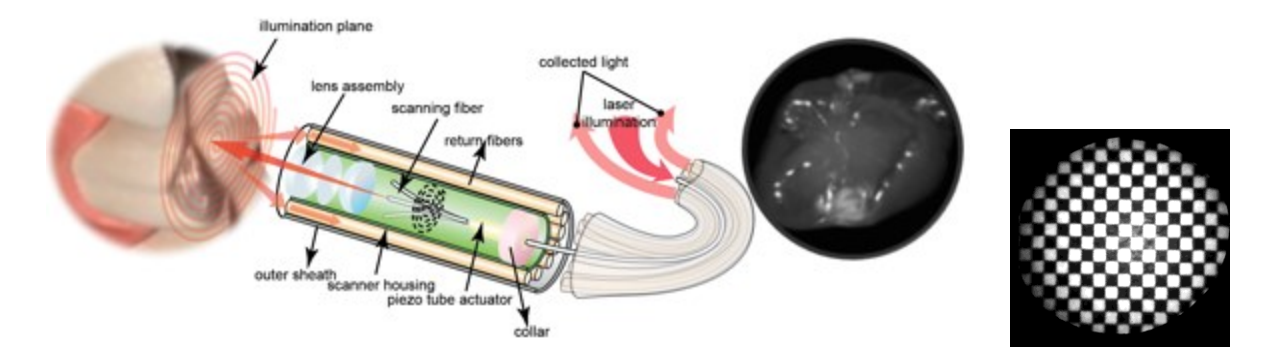


Fig. 2 (left) Schematics of near-infrared scanning fiber endoscope (nirSFE) which is drawn off scale to display functionality. Note that the middle image on the illumination plane is from the occlusal side of an extracted human tooth at 1460 nm illumination. (right) Falloff of brightness from the nirSFE 1310 nm image is displayed using checkerboard target of 1 mm squares.

Due to the Lambertian reflection law as well as the 0.5 numerical aperture of the return fibers, edge collection efficiency η_e which is the ratio of collected light scattered from the edge of FOV and all scattered light from the edge of FOV, is approximately 0.23 times of the center collection efficiency η_c . Falloff of collection efficiency limits the visible FOV, which reduces signal-to background ratio (contrast) at the border of FOV as shown in Fig. 2(b). The image resolution is limited by Gaussian beam spot size, number of scanning spirals and total number of pixels. Tested on USAF-1951 target (MIL-STD-150A), nirSFE has resolution of 140 μ m with a working distance of 20 mm. By moving the probe closer to the target, the resolution can be improved to 35 μ m with a working distance of 2 mm.

3 Methodology

A total of nineteen artificial interproximal lesions are created in five extracted human posterior teeth. Cavitation was prepared on the mesial or distal surface with a 330 carbide bur using a high-speed handpiece, and the cavities were filled with hydroxyapatite powder (P316R-CAPTAL R, Plasma Biotal Limited, Derbyshire, UK) and sealed with cyanoacrylate resin. Lesions are prepared at varying depth from occlusal surface from 1.43 mm to 3.45 mm, varying axial lesion depths to pulp from 0.58 mm to 3.35 mm (maximum depth of drilling), and varying lesion diameter varying from 0.5 mm to 2.28 mm. All lesions were not visible from the occlusal surface when teeth are mounted on a black Delrin® block for nirSFE imaging in air.

Because of the miniature size and flexibility, nirSFE probe can image from multiple perspectives, for example, from occlusal side or from buccal or lingual side with varying angulation, as shown in Fig. 3. Videos are acquired by a trained user from both occlusal side and buccal side of the teeth with frames selected for this report. Micro-CT (X5000, North Star Imaging, Minnesota) 3D

reconstructions were acquired by a trained engineer on these teeth to serve as the gold standard for measurement of lesion location and size. Pre-commercial 1310-nm swept source OCT (Yoshida Dental Mfg., Tokyo, Japan) with 110-nm band and 50-kHz scan rate are also used by a trained clinician to acquire 3D scans of the teeth from the occlusal views with a $10 \times 10 \times 8 \text{ mm}^3$ imaging range, and 11 µm axial resolution. Analyses of microCT data and OCT data were done using AmiraTM software. Since artificial interproximal lesions are separated from each other, one microCT slice may not contain all lesions. Furthermore, it was difficult to match nirSFE images with the cross-section slices, which lack surface topology. The microCT slices within selected range were superimposed to display lesions of interest for the convenience of displaying tooth surface topology and accurate matching of the lesions. Other useful small features, such as natural occlusal lesions found on these extracted teeth, were identified by aligning the crosshairs on 3D microCT view and then inspecting the corresponding cross-section slice.

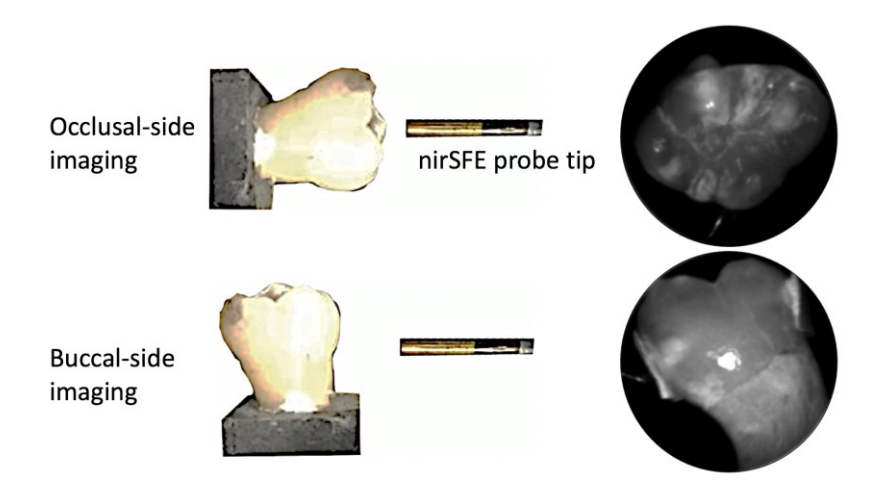


Fig. 3 Schematics of nirSFE imaging interproximal lesion (top) from occlusal side and (bottom) from buccal side of the tooth with 1310 nm light. Images of two imaging modes are on the right.

4 Results

Nineteen artificial interproximal lesions are inspected by occlusal-side nirSFE imaging. Diagnosis from a trained user by looking at real-time nirSFE videos indicates sensitivity of 78.9% (15 true

positives and 4 false negatives out of 19 lesions, not blinded). Clinicians were asked to inspect both presence and location of lesions. Since no clinicians marked any false positives on sound regions of teeth, the true negative rate in this study is 100%. Diagnosis from two dental clinicians by looking at saved nirSFE videos and/or video selected video frames indicates sensitivity (true positive rate) of 68.4% (13 true positives and 6 false negatives out of 19 lesions, not blinded) and 63.2% (12 true positives and 7 false negatives out of 19 lesions, blinded). Between two clinician examiners, the kappa statistic reached 80.3% which satisfies the minimum acceptable interrater agreement of 80%. The higher sensitivity from trained user may result from the advantage of real-time videos which provide more information than saved videos and snapshots who could detect all interproximal lesions under less than 4-mm-thick enamel layer. Clinicians were also asked to inspect both existence and location of lesions according to OCT images, the true positive rate and true negative rate are both 100%.

Figure 4 and Fig. 5 show two examples of samples and the corresponding images from three different modalities. Lesions show up as increased intensity within nirSFE reflectance images and OCT images since lesions scatter more light than sound enamel. In contrast, lesions appear dark in microCT scan due to reduced mineral content. 1310-nm nirSFE image captures the contour and surface of tooth, which can be beneficial when matching different imaging modalities and locating lesions, while 1460-nm nirSFE image provides higher contrast between lesion and sound enamel. In Fig. 4, the tooth has a dentin lesion and an enamel lesion on opposing interproximal surfaces. The enamel lesion and dentin lesion are clearly seen in both nirSFE images using 1310-and 1460-nm and OCT scans at 1310-nm. Due to the attenuation of NIR light, OCT can only detect the occlusal border of the advanced interproximal dentinal lesion, but gingival extent of the interproximal lesion is unresolved. When nirSFE and OCT were used for buccal-side imaging, the

occluso-gingival aspect of lesion could be evaluated. Similar to nirSFE, OCT scan also suffers from distortion caused by varying enamel thickness and birefringence of enamel prisms. The red, orange and yellow dashed circles in Fig. 4 and Fig. 5 indicate natural occlusal lesions which are detected by both nirSFE and OCT, and confirmed with microCT.

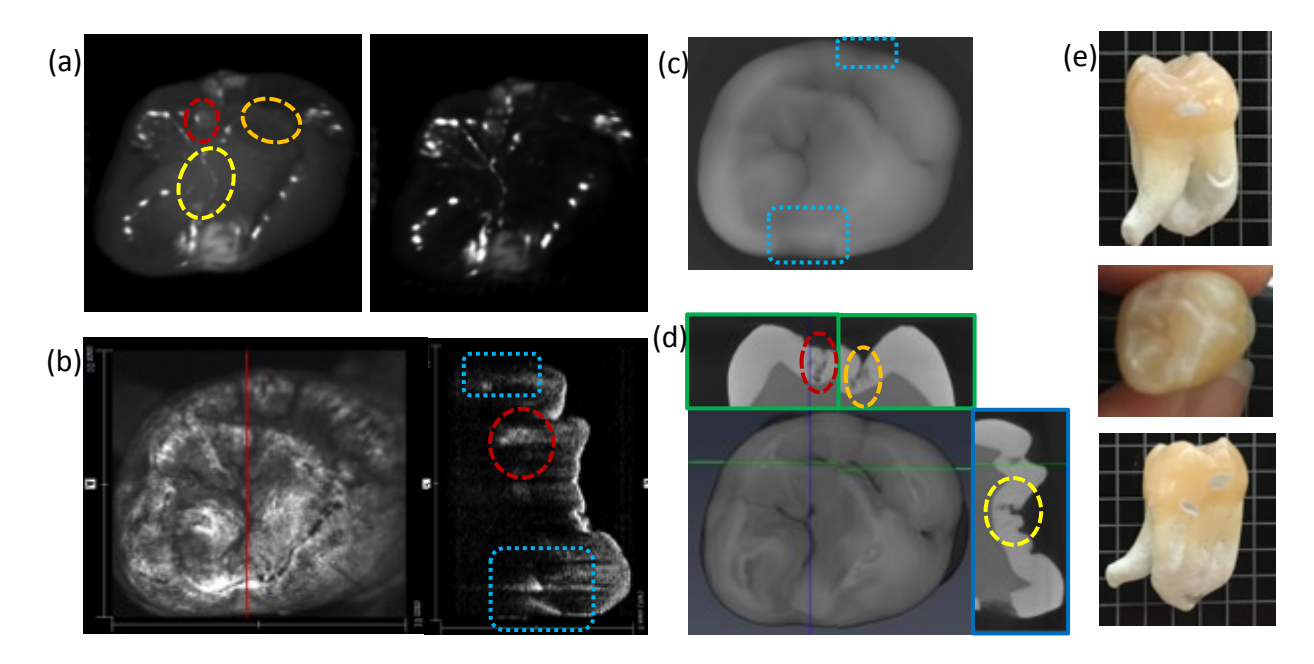


Fig. 4 Comparison of different modalities imaging on a tooth with a dentin lesion and an enamel lesion on each interproximal surface. (a) Occlusal-side nirSFE images using 1310nm laser diode (left) and 1460nm laser diode (right). (b) OCT b scan taken at the red line. (c) Superimposition of microCT slices. Note that the range of superimposed slices is chosen so that visibility of lesions matches the nirSFE image. (d) Micro-CT 3D view and 2D slices which contain natural occlusal lesions. (e) Visible light images of occlusal surface and two interproximal surfaces of the tooth. Note that the blue dashed frames indicate the artificial interproximal lesions and the red, orange and yellow dashed circles indicate natural occlusal lesions.

In Fig.5, we observe a tooth with three dentin lesions with various axial depths and four dentin lesions with various diameters on each interproximal surface. The left two lesions (One has a depth of 3.45 mm under the occlusal surface which is the largest among all 19 lesions, the other one has a diameter of 0.50 mm which is the smallest among all 19 lesions) are not detectable with nirSFE, while they were detected with OCT. The lesions that are under cusps are usually more difficult to detect using nirSFE due to thicker enamel layer on occlusal surface and a prominent cusp, which can be imaged more closely from another perspective, i.e. interproximal surfaces from buccal or

lingual perspective, where the lesion can be imaged through thinner enamel layer. In addition, we found several natural occlusal lesions on the tooth which were confirmed in microCT and observed using nirSFE and OCT, see red and yellow circles.

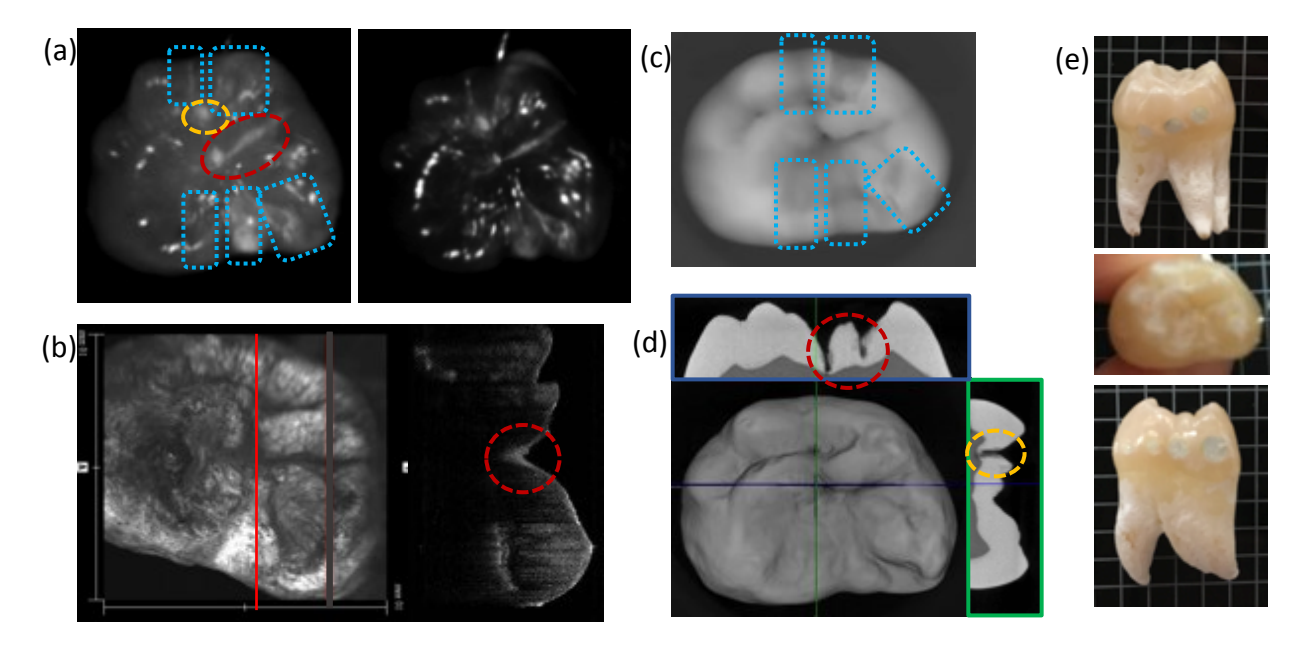


Fig. 5 Comparison of different modalities imaging on a tooth with three dentin lesions with various axial depth and four dentin lesions with various diameter on each interproximal surface. (a) Occlusal-side nirSFE images using 1310nm laser diode (left) and 1460nm laser diode (right). (b) OCT b scan taken at the red line. (c) Superimposition of microCT slices. Note that range of superimposed slices is chosen so that visibility of lesions matches the nirSFE image. (d) Micro-CT 3D view and 2D slices which contain natural occlusal lesions. (e) Visible light images of occlusal surface and two interproximal surfaces of the tooth. Note that the blue dashed frames indicate the artificial interproximal lesions and the red and orange dashed circles indicate natural occlusal lesions.

In both Fig. 4(a) and Fig. 5(a), there are specular reflection patterns in the nirSFE images which can look similar to the signal patterns from lesions. However, specular reflection patterns usually appear on glossy and curved surfaces like cusp tips where natural caries lesions rarely form. Also, interproximal lesions viewed from occlusal side have lower intensity than the saturated specular reflection patterns. Because occlusal lesions usually form in the pits and fissures on the occlusal surface, clinicians who are familiar with tooth anatomy and dental diagnostics can easily distinguish between specular reflection patterns and lesion signals.

The occlusal-side nirSFE image shows the diameter and axial depth to pulp of the interproximal lesions while the buccal- or lingual-side nirSFE images show the occluso-gingival aspect of lesions. Figure 6 shows an example of samples inspected by buccal-side nirSFE imaging. From the buccal side, the NIR light can penetrate through enamel and more light is scattered back by the nearest lesion (indicated by the blue dashed frame) and generate a bright pattern in the image which resolves the position and size of the lesion. The blue arrows indicate enamel defect on the border between enamel and root.

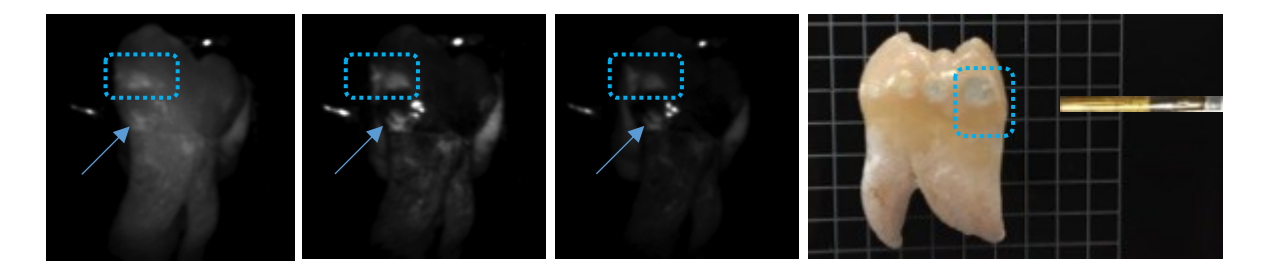
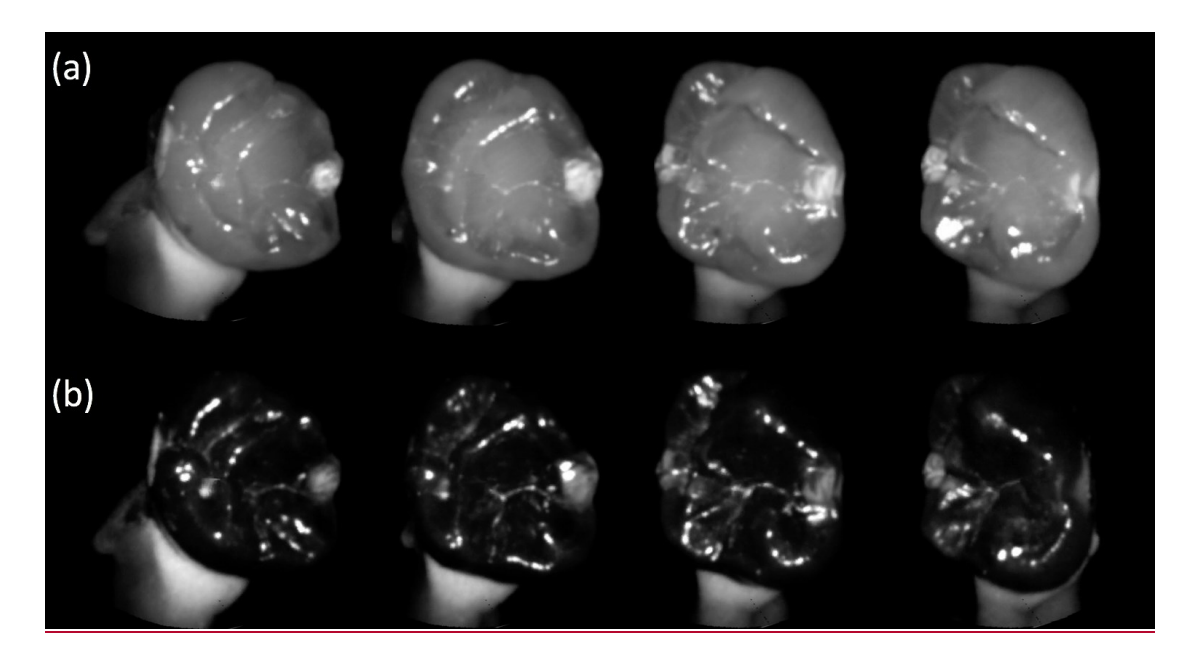


Fig. 6 In the (right) visible light image, the interproximal lesion noted by blue dashed frame can be captured clearly by (left) nirSFE imaging from buccal side using (from left to right) 1310nm, 1460nm and 1550nm laser diodes. Note that the arrows indicate surface calculus which also appears bright in NIR images.

5 Discussion and Conclusion

In summary, we developed a multispectral nirSFE based on scanning fiber endoscope which may lead to the smallest InGaAs-based camera with low cost for pediatric dentistry. Using a lab-bench prototype nirSFE system we conducted the first comparison study on imaging of nineteen artificial interproximal lesions as well as some natural occlusal lesions on extracted human teeth, a prototype OCT and a microCT as gold standard. The cross-sectional and 3D views of the prototype OCT system showed highest sensitivity while the nirSFE was able to detect lesions less than 4mm below the occlusal surface without false positives in a pilot study of 19 teeth. Prototype dental OCT systems even at 1310 nm for 932 teeth do have difficulty diagnosing caries below 2 mm in depth¹⁷. In general, clinical OCT systems are complex and costly, and may require larger probe size and operator skill to cover a wide range of views¹⁸. In contrast, nirSFE systems are less complex and real-time multispectral video systems can be produced at lower cost. Video recordings of nirSFE imaging occlusal side of extracted tooth with two artificial lesions at 1310 nm and 1460 nm are provided as supplemental information Video 1.



Video 1 Snapshots of nirSFE videos on occlusal side of the same extracted tooth with one artificial lesion on left and right sides at (a) 1310 nm and (b) 1460 nm (two MP4 files, 1.1 MB each). The two videos show the same tooth rotating from right side to left side. Note that as the tooth rotates, contrast of lesions changes and also specular reflection patterns move. Thus, real-time video has greater potential in detecting lesions and distinguishing them in presence of specular reflection.

Although not directly compared, commercial NIR-camera-based dental imaging systems use wavelengths below 900nm so that inexpensive small silicon-based cameras can be used. However, these wavelengths have 10 times higher optical scattering coefficient than 1200-1800nm which may limit its imaging depth and diagnostic accuracy^{19,20}. Current 1200-1800-nm NIR imaging requires InGaAs-based pixel-array cameras which are bulky and expensive²¹. With a diameter of less than 2 mm, the nirSFE can be placed within a hand instrument for pediatric dentistry²², and capture images in multiple perspectives around a tooth for better lesion detection.

In our previous work, we demonstrated nirSFE can detect both shallow artificial and natural occlusal lesions on extracted human teeth^{23,24}. From this study along with previous works, we conclude that nirSFE has significant potential in detecting occlusal lesions and interproximal lesions covered by less than 4mm enamel layer, which cannot be seen by visual inspection. The multispectral imaging capability which provides molecular-based absorption contrast from

multiple perspectives allowed by the small probe tip on the flexible shaft can provide a low-cost indication for a follow-up X-ray image. Future application can be monitoring these lesions heal over time with new remineralization therapies²⁵, possibly applied and monitored at home with a low-cost portable system. Finally, due to notable absorption features tissue constituents such as water, lipids and collagen in the range of 1000-2000nm wavelength, the nirSFE could play an important role in other health-related fields, including the characterization of conditions such as atherosclerotic plaque, breast cancer, and burns²⁶.

Disclosures

YZ and EJS are co-authors of patent filings owned by the University of Washington.

Acknowledgments

We acknowledge the funding support from National Institutes of Health NIDCR R21DE025356, NSF 1631146 Partnerships for Innovation and the UW School of dentistry fellowship program. We thank Cathy Olivio and Mattew Carson for technical support on nirSFE system fabrication and testing. We also thank Michelle Hickner for technical support on microCT scanning and image reconstruction of teeth samples. UW senior student Minh Tran designed and fabricated the tooth holder for microCT imaging which was funded by NSF MRI award #1428436.

References

1. N. J. Kassebaum, E. Bernabe, M. Dahiya, B. Bhandari, C.J.L.Murray, and W. Marcenes, "Global burden of untreated caries: a systematic review and metaregression," *J. Dent. Res.* **94**(5), 650-8 (2015) 2. N. Shah, N. Bansal, and A. Logani, "Recent advances in imaging technologies in dentistry," *World J. Radiol.* **6**(10), 794-807 (2014)

- 3. L. Karlsson and S. Tranaeus, "Supplementary methods for detection and quantification of dental caries," *J. Laser Dent.* **16**(1), 8-16 (2008)
- 4. L. Karlsson, "Caries detection methods based on changes in optical properties between healthy and carious tissue," *Int. J. Dent.* **2010**, 270729 (2010)
- 5. F. Javed and G. E. Romanos, "A comprehensive review of various laser- based systems used in early detection of dental caries," *Stoma Edu. J.* **2**(2), pp. 106–111 (2015)
- 6. D. Fried, J. D. B. Featherstone, C. L. Darling, R. S. Jones, P. Ngaotheppitak, and C. M. Buhler, "Early caries imaging and monitoring with near-infrared light,", *Dent Clin N Am* **49**, 771-793 (2005)
- 7. R. S. Jones and D. Fried, "Attenuation of 1310- and 1550-nm laser light through sound dental enamel," *Proc. SPIE 4610*, Lasers in Dentistry VIII (2002)
- 8. D. Fried, R. E. Glena, J. D. Featherstone, and W. Seka, "Nature of light scattering in dental enamel and dentin at visible and near-infrared wavelengths," *Appl. Opt.* **34**(7), 1278–1285 (1995)
- 9. G. M. Hale and M. R. Querry, "Optical constants of water in the 200 nm to 200 μm wavelength region," *Appl. Opt.* **12**(3), 555–563 (1973)
- 10. C. L. Darling, G. Huynh, and D. Fried, "Light scattering properties of natural and artificially demineralized dental enamel at 1310 nm," *Journal of Biomedical Optics* **11**(3), 034023:1–11 (2006)
- 11. J. Wu and D. Fried, "High contrast near-infrared polarized reflectance images of demineralization on tooth buccal and occlusal surfaces at 1310nm," *Lasers Surg. Med.* **41**(3), 208-213 (2009)
- 12. S. Chung, D. Fried, M. Staninec, and C. L. Darling, "Multispectral near-IR reflectance and transillumination imaging of teeth," *Biomedical optics express* **2**(10), 2804-2814 (2011)
- 13. W. A. Fried, D. Fried, K. H. Chan, and C. L. Darling, "High contrast reflectance imaging of simulated lesions on tooth occlusal surfaces at near-IR wavelengths," *Lasers Surg. Med.* **45**(8), 533–541 (2013)
- 14. J. C. Simon, S. A. Lucas, M. Staninec, H. Tom, K. H. Chan, C. L. Darling, and D. Fried, "Transillumination and reflectance probes for in vivo near-IR imaging of dental caries," *Proc. Of SPIE: Lasers in Dentistry XX* **8929**, 89290D-1-7 (2014)

- 15. C. S. Lee, D. C. Lee, C. L. Darling, and D. Fried, "Nondestructive assessment of the severity of occlusal caries lesions with near-infrared imaging at 1310 nm," *Journal of Biomedical Optics* **15**(4), 047011 (2010)
- 16. S. Chung, D. Fried, M. Staninec, and C. L. Darling, "Multispectral near-IR reflectance and transillumination imaging of teeth," *Biomed. Opt. Express* **2**(10), 2804-2814 (2011)
- 17. S. Mansour, J. Ajdaharian, T. Nabelsi, G. Chan, and P. Wilder-Smith, "Comparison of caries diagnostic modalities: a clinical study in 40 subjects," *Lasers. Surg. Med.* **48**, 924-928(2016)
- 18. M. J. Leahy, C. Wilson, J. Hogan, Peter O'Brien, R. Dsouza, K. Neuhaus, D. Bogue, H. Subhash, Colm O'Riordan, and Paul M. McNamara, "The how and why of a \$10 optical coherence tomography system," *Proc. SPIE 9697*, Optical Coherence Tomography and Coherence Domain Optical Methods in Biomedicine XX, 96970T (2016)
- 19. A. Jablonski-Momeni, B. Jablonski, and N. Lippe, "Clinical performance of the near-infrared imaging system VistaVam iX Proxi for detection of approximal enamel lesions," *BDJ open* **3**, 17012 (2017)
- 20. J. Khnisch, F. Schtig, V. Pitchika, R. Laubender, K. W. Neuhaus, A. Lussi, and R. Hickel, "In vivo validation of near-infrared light transillumination for interproximal dentin caries detection," *Clin. Oral Investig.* **20**(4), 821–829 (2016)
- 21. J. C. Simon, S. A. Lucas, M. Staninec, H. Tom, K. H. Chan, C. L. Darling, and D. Fried. (2014) Transillumination and reflectance probes for in vivo near-IR imaging of dental caries. Lasers in Dentistry XX, Proc. SPIE vol. 8929.
- 22. A. L. Rugg, L. Y. Nelson, M. A. I. Timoshchuk, and E. J. Seibel, "Design and fabrication of a disposable dental handpiece for clinical use of a new laser-based therapy-monitoring system," *J. Med. Devices* **10**(1), 011005 (2015)
- 23. E. J. Seibel, Y. Zhou, J. Y. Graham, L. Y. Nelson, "Optical dental care for children, from caries prediction to therapy monitoring," *OSA Biophotonics Conference proceedings*, Hollywood, FL, April 3-6, paper#CTh4B.2 (2018)

- 24. Y. Zhou, R. Lee, A. Sadr, and E. J. Seibel, "Near-infrared dental imaging using scanning fiber endoscope," *Lasers in Dentistry XXIV, Proc. SPIE* 10473, 1047308 (2018)
- 25. S. R. Jefferies, "Advances in remineralization for early carious lesions: a comprehensive review," *Compend. Contin. Educ. Dent.* **35**(4), 237-43 (2014)
- 26. R. H. Wilson, K. P. Nadeau, F. B. Jaworski, B. J. Tromberg, and A. J. Durkin, "Review of short-wave infrared spectroscopy and imaging methods for biological tissue characterization," *J Biomed Opt.* **20**(3), 030901 (2015)

Caption List

- Fig. 1 Attenuation coefficient of light in dental enamel layer and water.
- **Fig. 2** (a) Schematics of near-infrared scanning fiber endoscope which is drawn off scale to display details better. Note that the image on the illumination plane is the SFE image from the occlusal side of an extracted human tooth. (b) Falloff of brightness of an nirSFE image of checkerboard target.
- **Fig. 3** Schematics of nirSFE imaging interproximal lesion (top) from occlusal side and (bottom) from buccal side of the tooth. Images of two imaging modes are on the right.
- **Fig. 4** Comparison of different modalities imaging on a tooth with a dentin lesion and an enamel lesion on each interproximal surface. (a) Occlusal-side nirSFE images using 1310nm laser diode (left) and 1460nm laser diode (right). (b) OCT b scan taken at the red line. (c) Superimposition of microCT slices. Note that the range of superimposed slices is chosen so that visibility of lesions matches the nirSFE image. (d) Micro-CT 3D view and 2D slices which contain natural occlusal lesions. (e) Visible light images of occlusal surface and two interproximal surfaces of the tooth. Note that the blue dashed frames indicate the artificial interproximal lesions and the red, orange and yellow dashed circles indicate natural occlusal lesions.

Fig. 5 Comparison of different modalities imaging on a tooth with three dentin lesions with various axial depth and four dentin lesions with various diameter on each interproximal surface. (a) Occlusal-side nirSFE images using 1310nm laser diode (left) and 1460nm laser diode (right). (b) OCT b scan taken at the red line. (c) Superimposition of microCT slices. Note that range of superimposed slices is chosen so that visibility of lesions matches the nirSFE image. (d) Micro-CT 3D view and 2D slices which contain natural occlusal lesions. (e) Visible light images of occlusal surface and two interproximal surfaces of the tooth. Note that the blue dashed frames indicate the artificial interproximal lesions and the red and orange dashed circles indicate natural occlusal lesions.

Fig. 6 In the (right) visible light image, the interproximal lesion noted by blue dashed frame can be captured clearly by (left) nirSFE imaging from buccal side using (from left to right) 1310nm, 1460nm and 1550nm laser diodes. Note that the arrows indicate surface calculus which also appears bright in NIR images.

Video 1 Snapshots of nirSFE videos on occlusal side of the same extracted tooth with one artificial lesion on left and right sides at (a) 1310 nm and (b) 1460 nm (two MP4 files, 1.1 MB each). The two videos show the same tooth rotating from right side to left side. Note that as the tooth rotates, contrast of lesions changes and also specular reflection patterns move. Thus, real-time video has greater potential in detecting lesions and distinguishing them in presence of specular reflection.